

## Activation of RGS9-1GTPase Acceleration by Its Membrane Anchor, R9AP\*

Received for publication, November 26, 2002, and in revised form, January 17, 2003  
Published, JBC Papers in Press, January 30, 2003, DOI 10.1074/jbc.M212046200

Guang Hu, Zhixian Zhang, and Theodore G. Wensel‡

From the Department of Biochemistry and Molecular Biology, Baylor College of Medicine, Houston, Texas 77030

The GTPase-accelerating protein (GAP) complex RGS9-1-G $\beta_5$  plays an important role in the kinetics of light responses by accelerating the GTP hydrolysis of G $\alpha_t$  in vertebrate photoreceptors. Much, but not all, of this complex is tethered to disk membranes by the transmembrane protein R9AP. To determine the effect of the R9AP membrane complex on GAP activity, we purified recombinant R9AP and reconstituted it into lipid vesicles along with the photon receptor rhodopsin. Full-length RGS9-1-G $\beta_5$  bound to R9AP-containing vesicles with high affinity ( $K_d < 10$  nM), but constructs lacking the DEP (dishevelled/EGL-10/pleckstrin) domain bound with much lower affinity, and binding of those lacking the entire N-terminal domain (*i.e.* the dishevelled/EGL-10/pleckstrin domain plus intervening domain) was not detectable. Formation of the membrane-bound complex with R9AP increased RGS9-1 GAP activity by a factor of 4. Vesicle titrations revealed that on the time scale of phototransduction, the entire reaction sequence from GTP uptake to GAP-catalyzed hydrolysis is a membrane-delimited process, and exchange of G $\alpha_t$  between membrane surfaces is much slower than hydrolysis. Because in rod cells different pools exist of RGS9-1-G $\beta_5$  that are either associated with R9AP or not, regulation of the association between R9AP and RGS9-1-G $\beta_5$  represents a potential mechanism for the regulation of recovery kinetics.

Timely deactivation of G protein  $\alpha$  subunits is a key element of responses to the stimulation of G protein-coupled receptors. It plays an especially important role in fast cellular responses such as those of vertebrate photoreceptors. In the rod and cone cell outer segments, the recovery phase of light responses depends on the presence of a GTPase-accelerating protein (GAP)<sup>1</sup> complex RGS9-1-G $\beta_5$  (1–4). Whether and how the GAP activity of this complex is regulated is unknown.

RGS9-1 contains multiple functional domains, including an RGS domain that is responsible for its GAP activity (3), a G protein  $\gamma$  subunit-like domain for G $\beta_{5L}$  binding (4, 5), an N-terminal domain that includes a DEP (dishevelled/EGL-10/pleckstrin) domain (6) and an intermediate domain (7), and a

C-terminal domain that is unique to RGS9-1 among all of the RGS proteins (8). All of these domains have been found to participate in the regulation of GAP activity and substrate specificity (9–11). The inhibitory PDE $\gamma$  subunit of the effector regulated by G $\alpha_t$ , cGMP phosphodiesterase (PDE6), interacts with both G $\alpha_t$  and the catalytic core of RGS9-1 and enhances RGS9-1 GAP activity (12–14) *in vitro*, but it is not clear how this enhancement is accomplished in a physiological setting in which tight PDE $\gamma$  binding to PDE6 catalytic subunits blocks GAP enhancement (15–18).

Additional possible mechanisms for regulation include a light- and calcium-regulated phosphorylation (19, 20) of RGS9-1 and interactions with the recently discovered membrane anchor protein, R9AP (7, 21). R9AP is a 25-kDa protein that is selectively expressed in photoreceptor outer segments. Homologues are apparent in genomic sequence from mouse (GenBank<sup>TM</sup> accession number NW\_000311), human (GenBank<sup>TM</sup> accession number NT\_011196), rat (GenBank<sup>TM</sup> accession number AC128498), zebra fish (NCBI trace archive numbers 15766910 and 46042404), and puffer fish (GenBank<sup>TM</sup> accession numbers CAAB01004012 and CAAB01001872), and in expressed sequence tags from human (GenBank<sup>TM</sup> accession numbers AW302149 and BQ187216), mouse (GenBank<sup>TM</sup> accession numbers BB591662 and BU506122), *Xenopus* (GenBank<sup>TM</sup> accession number BG515592), and zebra fish (GenBank<sup>TM</sup> accession number BE015922). R9AP contains a single transmembrane  $\alpha$  helix, and sequence analysis suggests structural similarity to the syntaxin family of proteins involved in membrane targeting (for a review on syntaxin family proteins, see Ref. 22). Biochemical assays and colocalization on co-expression in cell culture indicate that it acts as a membrane anchor for RGS9-1-G $\beta_5$ , which binds to the cytoplasmic domain of R9AP (21). The molar ratio of R9AP to RGS9-1 in bovine rod outer segments appears to be variable and was found to range from 0.4 to 0.8. Consistent with these ratios, co-immunoprecipitation experiments revealed that whereas all detectable R9AP in the retina is bound to RGS9-1-G $\beta_5$ , a distinct pool of RGS9-1-G $\beta_5$  is not associated with R9AP. Here we describe experiments with recombinant R9AP reconstituted into lipid vesicles, which demonstrate that binding of RGS9-1-G $\beta_5$  to membrane-anchored R9AP dramatically enhances its GAP activity toward G $\alpha_t$ .

### EXPERIMENTAL PROCEDURES

**Buffers**—Standard buffers were: GAPN buffer: 100 mM NaCl, 2 mM MgCl<sub>2</sub>, and 10 mM HEPES, pH 7.4; ConA buffer: 300 mM NaCl, 50 mM Tris-HCl, pH 7.0, 1 mM CaCl<sub>2</sub>, 1 mM MgCl<sub>2</sub>, and 1 mM MnCl<sub>2</sub>; lysis buffer: 300 mM NaCl and 25 mM Tris-HCl, pH 8.0; and high-salt buffer: 10 mM HEPES, 1 M NH<sub>4</sub>Cl, and 2 mM MgCl<sub>2</sub>. For all these buffers, 1 mM dithiothreitol and ~20 mg/liter solid phenylmethylsulfonyl fluoride were added before use.

**Protein Electrophoresis and Immunoblotting**—SDS-PAGE and immunoblotting were carried out using standard protocols (23). Rabbit

\* This work was supported by NEI, National Institutes of Health and the Welch Foundation. The costs of publication of this article were defrayed in part by the payment of page charges. This article must therefore be hereby marked "advertisement" in accordance with 18 U.S.C. Section 1734 solely to indicate this fact.

‡ To whom correspondence should be addressed: Dept. of Biochemistry and Molecular Biology, Baylor College of Medicine, One Baylor Plaza, Houston, Texas 77030. Tel.: 713-798-6996; Fax: 713-798-1625; E-mail: twensel@bcm.tmc.edu.

<sup>1</sup> The abbreviations used are: GAP, GTPase-accelerating protein; RGS, regulator of G protein signaling; ROS, rod outer segments; R9AP, RGS9-1 anchor protein; PDE $\gamma$ , phosphodiesterase  $\gamma$  subunit; ConA, concanavalin A; GST, glutathione S-transferase.

anti-RGS9-1c polyclonal antiserum was generated as described previously and was used at a dilution of 1:1000. The secondary antibodies used were horseradish peroxidase-conjugated (Promega) anti-rabbit antibody, with detection by chemiluminescence using the ECL<sup>®</sup> system (Amersham Biosciences).

**Expression and Purification of R9AP**—His-tagged bovine R9AP cytoplasmic domain (His-bR9AP-ΔC, amino acids 1–212, previously named His-bp25-ΔC) and His-tagged full-length murine R9AP (His-mR9AP) were expressed in *Escherichia coli* using plasmids and procedures described previously (21), and His-bR9AP-ΔC was purified as described. For His-mR9AP purification, the cells were collected and lysed in lysis buffer by sonication on ice, and insoluble proteins including His-mR9AP were separated from soluble proteins by centrifugation at  $24,000 \times g$  at 4 °C in a Beckman JA 25.50 rotor. The insoluble proteins were extracted with 4% sodium cholate (3 $\alpha$ ,7 $\alpha$ ,12 $\alpha$ -trihydroxy-5 $\beta$ -cholanic acid, sodium salt, Sigma) in lysis buffer for ~30–60 min at 4 °C with gentle agitation, and the proteins in the supernatant were separated from the pellet by centrifugation. The extraction was repeated a total of 3–4 times, yielding > 70% of total His-mR9AP extracted in soluble form. The detergent supernatants were pooled together, and His-mR9AP was purified by nickel nitrilotriacetic (Ni-NTA superflow, Qiagen) chromatography in 4% sodium cholate in lysis buffer according to the manufacturer's protocol to obtain His-mR9AP of >95% purity.

**Expression and Purification of RGS9-1-G $\beta_5$** —GST-tagged RGS9-1 (amino acids 1–484)-G $\beta_5$ , RGS9-1-NGD (amino acids 1–431)-G $\beta_5$ , and His-tagged RGS9-1-IGRC (amino acid 112–484)-G $\beta_5$  complex were expressed and purified from Sf9 cells as described previously (9, 11). GST-tagged RGS9-1-D (amino acid 276–431) was expressed and purified from *E. coli* as described previously (14).

**Rhodopsin Purification**—Bovine ROS were purified as described previously (25). Rhodopsin was purified from bovine ROS according to the protocol described previously with modifications (26). Briefly, ROS membranes were extracted in the dark with high salt buffer twice to remove soluble protein contaminants and then washed with ConA buffer and pelleted. Pelleted membranes were solubilized in 4% sodium cholate in ConA buffer, and insoluble material was removed by centrifugation. Concanavalin A immobilized on Sepharose beads was first cross-linked in 0.05% glutaraldehyde in 250 mM NaHCO<sub>3</sub> at room temperature for ~2 h to prevent loss of immobilized concanavalin A and then prepared as described previously (26). Rhodopsin was eluted with 300 mM  $\alpha$ -methyl-mannoside in 4% sodium cholate in ConA buffer. The sealed column and 1.5-column volumes of elution buffer were gently agitated at 4 °C for 20–30 min, and then the eluted protein was drained from the column. This procedure was repeated twice, and the eluted proteins were pooled together and concentrated in a protein concentrator (Millipore) to obtain a final rhodopsin concentration (determined by dark absorbance at 500 nm) of 2–3 mg/ml.

**Vesicle Reconstitution**—Lipids used for vesicle reconstitution were L- $\alpha$ -phosphatidylserine (brain and porcine-sodium salt), L- $\alpha$ -phosphatidylcholine and (egg and chicken), L- $\alpha$ -phosphatidylethanolamine (egg and chicken) from Avanti Polar Lipids. Lipids were mixed at a ratio (w/w) of phosphatidylcholine:phosphatidylethanolamine:phosphatidylserine = 50:35:15 in chloroform, dried under argon flow, and redissolved in 4% sodium cholate in lysis buffer to a final concentration of 20 mg/ml. In the lipid-only vesicles (see below) and R9AP vesicles that were used in binding assays, rhodamine-labeled phosphatidylethanolamine (Molecular Probes Inc., N-(6-tetramethylrhodaminethiocarbonyl)-1,2-dihexadecanoyl-sn-glycero-3-phosphoethanolamine, triethylammonium salt) was added in the lipid mixture to a final concentration of 0.5% (w/w) to facilitate the visualization of the lipids. Detergent-solubilized lipids were then mixed with purified proteins (rhodopsin, His-mR9AP, or rhodopsin and His-mR9AP) at a lipid-to-protein (w/w) ratio of 20–40:1 and dialyzed against GAPN buffer (>100 $\times$  volume) for ~120 h with buffer changes every 20–24 h (27). Under these conditions, the majority of the proteins were incorporated into the vesicles. After dialysis, samples were collected and centrifuged at  $18,000 \times g$  in a Beckman TL100 rotor to remove aggregated proteins and lipids, and the vesicles in the supernatant were concentrated by one of the following two methods. For the purpose of vesicle binding assays, R9AP vesicles were pelleted by ultracentrifugation at  $88,000 \times g$  to collect easily pelleted vesicles, and vesicles that stayed in the supernatant were discarded. Pelleted vesicles were resuspended in GAPN buffer to the desired concentration by repeated extrusion through a 26-gauge needle. As a control for the binding assays, lipid-only vesicles without protein were made similarly in parallel. For the purpose of GAP assays the vesicles were concentrated in a protein concentrator (Millipore) to achieve the maximum yield. Lipid concentrations of the sam-

ples were determined by measuring the total phosphate concentrations using phosphorus assays (28). The molar vesicle concentrations were calculated using the following formula: molar concentration of vesicles = (formal concentration of phospholipids  $\times s$ )/ $4\pi r^2$ , where  $s$  is the average surface area of a phospholipid headgroup in Å<sup>2</sup> (70 Å<sup>2</sup>), and  $r$  is the average vesicle radius in Å. We used  $r = 272$  Å, which was derived from least squares fitting of the data in Fig. 4. This value is consistent with the appearance of the vesicles in electron micrographs (Fig. 1A,  $r = 240 \pm 50$  Å,  $n = 150$ ). The rhodopsin concentrations were determined by measuring the differential absorbance at 500 nm (using extinct coefficient =  $40,600 \text{ M}^{-1} \text{ cm}^{-1}$ ) of the sample dissolved in 1.5% lauryldimethylamine oxide before and after illumination. The R9AP concentrations were determined by densitometry of Coomassie-stained SDS-PAGE gels using bovine serum albumin as standard.

**Electron Microscopy**—The reconstituted vesicles in solution (vesicle concentration ~200–300 nM) were frozen across the holes of 400-mesh carbon-coated holey grids by rapid plunging into liquid ethane (29, 30). Electron microscopy was performed on a JEOL1200EX equipped with a Gatan liquid nitrogen specimen holder at 100 keV. Images were recorded at a nominal magnification of  $\times 40,000$  with a dose of ~20 electrons per Å<sup>2</sup> onto Kodak SO-163 photographic film developed for 12 min in Kodak D19 developer at 20 °C. Micrographs were digitized using a Zeiss Phodis SCIA microdensitometer at 14  $\mu\text{m}/\text{pixel}$ .

**Vesicle Binding Assay**—Purified RGS9-1 proteins (in GAPN buffer) were first centrifuged at  $88,000 \times g$  for 40 min to remove aggregates. Supernatants were diluted to desired concentrations in GAPN buffer containing 0.2 mg/ml ovalbumin, mixed with R9AP vesicles or lipid-only vesicles in a volume of 300  $\mu\text{l}$ , and incubated with gentle shaking at 4 °C for ~3 h. 150  $\mu\text{l}$  of the reaction mixture was then transferred to a new polypropylene tube (Beckman) to separate unbound proteins from bound proteins by pelleting the vesicles at  $88,000 \times g$  for 40 min. The pelleted vesicles were clearly visible as a pink pellet at the bottom of the tube because of the rhodamine tag. The final concentrations in the binding reactions were RGS9-1 proteins (GST-RGS9-1-G $\beta_5$ , His-RGS9-1-IGDC-G $\beta_5$ , GST-RGS9-1-NGD-G $\beta_5$ , or GST-RGS9-1-D), 0.1  $\mu\text{M}$ ; R9AP (total concentration), 3.0  $\mu\text{M}$ ; lipid (as an indication of vesicle concentration, measured by phosphate concentration), 0.8 mM. Equal proportions of the starting binding reactions, the supernatant after the vesicles were pelleted, and the pelleted vesicles were loaded on SDS-PAGE, and the RGS9 proteins were detected by immunoblotting using anti-RGS9-1c antiserum.

**Transducin Activation Assay**—Transducin activation by rhodopsin vesicles was determined as described previously (31). Briefly, rhodopsin or rhodopsin and R9AP vesicles were diluted in GAPN buffer and mixed with purified transducin in a volume of 192  $\mu\text{l}$  in dim red light. The reaction was initiated by the addition of 18  $\mu\text{l}$  of [ $\gamma$ -<sup>35</sup>S] GTP (specific activity = 400–500 Ci/mol) to the mixture, and 18  $\mu\text{l}$  of the reaction was removed and quenched on the filter membrane at the specified time points. The reactions were kept in dim red light until  $t = 3.0$  min and were exposed to room light starting from  $t = 3.0$  min until the end of the assays. The final concentrations in the assays were 1 nM rhodopsin, 0.5  $\mu\text{M}$  transducin, and 2.5  $\mu\text{M}$  [ $\gamma$ -<sup>35</sup>S]-GTP.

**Single Turnover GTPase Activity Assay**—Single turnover G $\alpha_t$  GTPase assays were carried out as described previously (9), and full-length His<sub>6</sub>-tagged PDE $\gamma$  (expressed and purified from *E. coli*) was added to enhance RGS9-1 GAP activity. Briefly, rhodopsin, rhodopsin and R9AP vesicles, or urea-washed ROS membranes were mixed with purified transducin and RGS9-1 proteins in GAPN buffer and incubated on ice for ~30 min. GTP hydrolysis was initiated by the addition of [ $\gamma$ -<sup>32</sup>P] GTP to the above mixture and was quenched by adding 5% trichloroacetic acid at various times. Phosphate released from hydrolyzed GTP was determined by activated charcoal assay. Final concentrations in the reactions using the reconstituted vesicles were 0.1  $\mu\text{M}$  RGS9-1 proteins and 0.2  $\mu\text{M}$  recombinant His<sub>6</sub>-PDE $\gamma$ ; final concentrations in the reactions using urea-washed ROS were 72  $\mu\text{M}$  rhodopsin, 1.0  $\mu\text{M}$  transducin, and 1.0  $\mu\text{M}$  recombinant His<sub>6</sub>-PDE $\gamma$ . The first order rate constant for GTP hydrolysis ( $k_{\text{inact}}$ ) was obtained by the fitting of data to single exponentials, and the rate constants were plotted as mean  $\pm$  S.D. In the reactions with urea-washed ROS, we used ROS membranes washed with either 4 M urea (32) or 6 M urea (7). Similar results were obtained on these two membranes. The difference was a slightly decreased  $k_{\text{cat}}/K_m$  value of RGS9-1-G $\beta_5$  on the membranes treated with 6 M urea that was probably caused by denaturation of some endogenous R9AP.

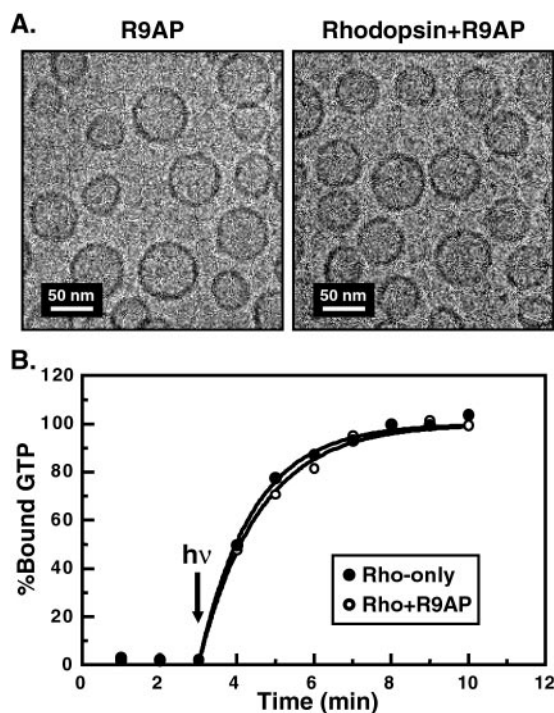


**FIG. 1. Vesicle reconstitution.** *A*, electron cryomicroscopy of reconstituted vesicles in vitreous ice. *R9AP*, R9AP-only vesicles; *Rhodopsin+R9AP*, rhodopsin and R9AP vesicles. *B*, rhodopsin activity on reconstituted vesicles measured by  $G_t$  [ $\gamma$ - $^{35}$ S] GTP uptake on light illumination. *Closed circles*, rhodopsin-only vesicles; *open circles*, rhodopsin and R9AP vesicles. Each sample contained 1 nM rhodopsin. The curves shown for data points after illumination are fits to single exponentials.

## RESULTS AND DISCUSSION

**Reconstitution of R9AP and Rhodopsin Vesicles**—Because R9AP has a transmembrane domain close to its C terminus, it is expressed as an insoluble protein in both *E. coli* and Sf9 cells (data not shown). Because the yield of *E. coli* expression ( $\sim 10$  mg/liter) is much better than that of Sf9 expression ( $\sim 0.5$  mg/liter), we used detergent extractions to purify R9AP expressed in *E. coli*. We tested both sodium cholate and dodecyl maltoside for their performance in extracting R9AP because of their compatibility with rhodopsin purification (26, 33), and we found that R9AP is readily extractable from the *E. coli*-expressed proteins by both detergents with comparable efficiency (data not shown). We therefore chose to use sodium cholate for our experiments for its lower cost. After further purification over the nickel-nitriloacetic acid column in the presence of detergent, R9AP was reconstituted into lipid vesicles using a conventional dialysis method. The composition of lipid headgroups used in the reconstitution was chosen to mimic that of mammalian rod outer segments (34). Dialysis yielded small unilamellar spherical vesicles of a fairly narrow size distribution ( $r = 240 \pm 50$  nm;  $n = 150$ ) (Fig. 1A). The functions of rhodopsin and R9AP on the vesicles were tested by transducin activation assays (Fig. 1B) and RGS9-1 binding (Fig. 2), respectively, and both proteins were found to be functional. The presence of R9AP in the vesicles had little effect on rhodopsin activity.

Although *E. coli* is overwhelmingly the most common heterologous expression system for mammalian proteins, and it generally provides the largest amounts of protein for the least expense, relatively few examples exist of successful purification and reconstitution of mammalian transmembrane proteins from bacteria (35). Our results provide an example of a successful strategy for the preparation in functional form of a

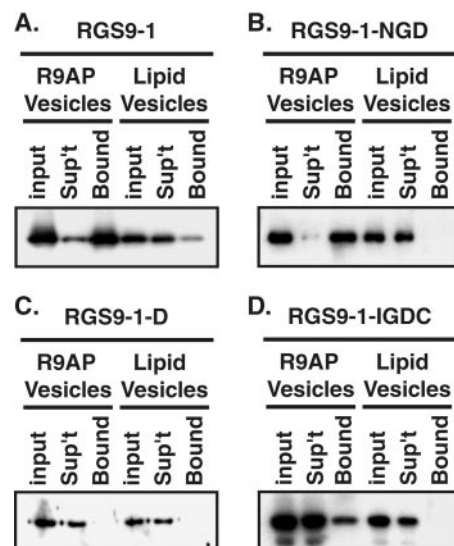


**FIG. 2. Membrane anchoring of RGS9-1 by R9AP.** The binding of GST-RGS9-1- $G\beta_5$  (*A*), GST-RGS9-1-NGD- $G\beta_5$  (*B*), GST-RGS9-1-D (*C*), and GST-RGS9-1-IGDC- $G\beta_5$  (*D*) to R9AP vesicles or lipid-only vesicles is shown. Equal proportions of the starting reaction containing the RGS9-1 proteins and the vesicles (*input*), the supernatant after pelleting the vesicles (*Sup't*), and the pelleted vesicles collected by resuspension (*Bound*) were separated by SDS-PAGE, and RGS9-1 proteins were detected by immunoblotting with chemiluminescence detection. Total GST-RGS9-1- $G\beta_5$  in the lipid-only samples is lower because of the loss of GST-RGS9-1- $G\beta_5$  to the walls of the reaction tubes.

protein with a relatively small cytoplasmic domain and a single transmembrane helix that may be applicable to additional proteins of this type.

**Membrane Anchoring of RGS9-1- $G\beta_5$  Complex by R9AP**—We have shown previously (21) that R9AP directly interacts with the RGS9-1 N-terminal domain. Here we tested whether RGS9-1 can be anchored to lipid vesicles by R9AP through this interaction (Fig. 2) by incubating recombinant RGS9-1 domain proteins with R9AP vesicles and removing the vesicles by centrifugation. We found that both the RGS9-1-NGD (amino acids 1–431)- $G\beta_5$  complex and RGS9-1 (amino acids 1–484)- $G\beta_5$  complex bound to the R9AP vesicles, whereas RGS9-1-IGDC (amino acids 112–484)- $G\beta_5$  bound much more weakly, and RGS9-1-D (amino acids 276–431) did not bind at all. The binding to lipid vesicles (Fig. 2A, lane 6) was very weak. Therefore, R9AP is sufficient to anchor RGS9-1 to the membranes by interacting with its N-terminal domain, and both the dishevelled/EGL-10/pleckstrin (DEP) domain and the intermediate domain of RGS9-1 are important for the binding, consistent with our previous findings (21). By titrating in full-length RGS9-1- $G\beta_5$  over a fixed concentration of R9AP vesicles in binding assays, we further determined that  $\sim 40\%$  of the total R9AP on the vesicles was able to bind RGS9-1- $G\beta_5$  (data not shown), suggesting that R9AP assumed a nearly random orientation in the vesicles during reconstitution.

**Membrane Anchoring of RGS9-1 by R9AP Enhances Its GAP Activity**—Lishko *et al.* (7) recently reported that association of the RGS9-1- $G\beta_5$  complex with high affinity sites on ROS membranes dramatically enhanced its GAP activity. To test the enhancement of GAP activity caused by membrane anchoring of the RGS9-1- $G\beta_5$  complex by R9AP, we measured the GAP activity of RGS9-1- $G\beta_5$  complex on reconstituted vesicles with defined protein compositions. We reconstituted purified rhodopsin with and without recombinant full-length R9AP in lipid vesicles and compared the GAP activity of RGS9-1 on these two vesicles. We found that the activity of RGS9-1 increased  $\sim 3$ – $4$ -fold on the rhodopsin and R9AP vesicles above that on the rhodopsin-only vesicles. The increase in activity occurred on

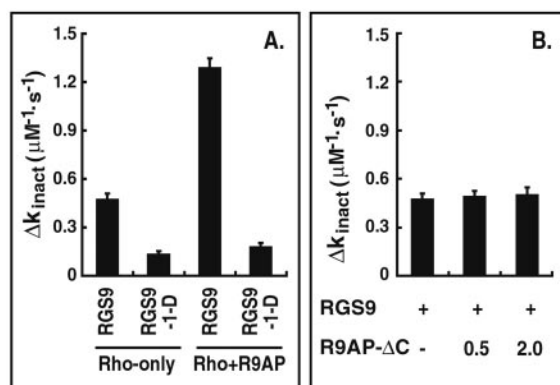


**FIG. 3. Enhancement of RGS9-1 GAP activity by R9AP membrane anchoring.** A, GTP hydrolysis rates for  $G_t$  reconstituted on vesicles containing rhodopsin only or rhodopsin and R9AP, in the presence of GST-RGS9-1- $G\beta_5$  (RGS9) or GST-RGS9-1-D (RGS9-1-D), were measured as described in the text. Final concentrations in the assays were: rhodopsin, 4.0  $\mu\text{M}$ ;  $G_t$ , 0.5  $\mu\text{M}$ ; RGS9-1 proteins, 0.1  $\mu\text{M}$ ; R9AP, 1.2  $\mu\text{M}$ ; vesicles, 96 nM (formal molar concentration of phospholipid divided by average number of phospholipids per vesicle). RGS9-1 GAP activity ( $\Delta k_{\text{inact}}$ ) on each vesicle was calculated as  $\Delta k_{\text{inact}} = k_{\text{inact}}$  (of  $G_t$  in the presence of RGS9-1)  $- k_{\text{inact}}$  (of  $G_t$ ). B, GTP hydrolysis rates on rhodopsin-only vesicles in the absence or presence of 0.1  $\mu\text{M}$  GST-RGS9-1- $G\beta_5$  (RGS9) and in the absence or presence of 0.5 or 2.0  $\mu\text{M}$  His-bR9AP- $\Delta\text{C}$  (R9AP- $\Delta\text{C}$ ) were measured by single turnover assays. Other protein and vesicle concentration were the same as in A.

the full-length RGS9-1- $G\beta_5$  complex that binds to R9AP but not on the RGS9-1-D protein that does not bind R9AP (Fig. 3A). Furthermore, the increase in activity was not merely because of the interaction between the R9AP-soluble domain and RGS9-1, because the addition of R9AP-soluble domain to rhodopsin-only vesicles had no effect on RGS9-1 activity (Fig. 3B). Therefore, we conclude that membrane anchoring of RGS9-1 by R9AP enhances RGS9-1 GAP activity, probably at least in part simply by localizing and orienting RGS9-1 on the vesicles.

To determine the maximal enhancement of GAP activity by the R9AP-containing vesicles, we performed a vesicle titration, holding the concentrations of RGS9-1- $G\beta_5$  constant. Under these conditions, the GAP activity of RGS9-1- $G\beta_5$  is expected to increase when the fraction of RGS9-1- $G\beta_5$  associated with R9AP increases. However, as the vesicle concentration increases at a constant RGS9-1- $G\beta_5$  concentration, a potential counteracting effect also occurs when the number of vesicles approaches and exceeds the number of RGS9-1- $G\beta_5$  complexes. In these conditions, an increase in the number of vesicles increases the probability of  $G\alpha_t$ -GTP formation on a vesicle lacking RGS9-1- $G\beta_5$ . Therefore, if  $G\alpha_t$ -GTP exchange between vesicles is very slow on the time scale of GTP hydrolysis, then at higher vesicle concentrations the apparent GAP activity must decline. Moreover, if  $G_t$  and RGS9-1- $G\beta_5$  bind to rhodopsin- and R9AP-containing vesicles independently of one another, the apparent GAP activity should decline in a way predicted by Poisson statistics. As shown in Fig. 4A, the behavior observed corresponds precisely to these expectations. The effect of titration in R9AP vesicles is biphasic, with GAP activity enhancement increasing at low concentrations and decreasing at higher vesicle concentrations. We were able to model the experimental results by theoretical calculations on the basis of the above considerations and another assumption that the dissociation coefficient ( $K_d$ ) between RGS9-1 and R9AP on the vesicles is much lower than the concentrations used in the experiments (*i.e.* all of the RGS9-1 could be anchored by available R9AP). The calculated -fold enhancement agreed very well with the experimental data (Fig. 4A, *fitted curve*), supporting the validity of the assumption and giving a maximum GAP enhancement of 4-fold. The declining activity at higher vesicle concentra-

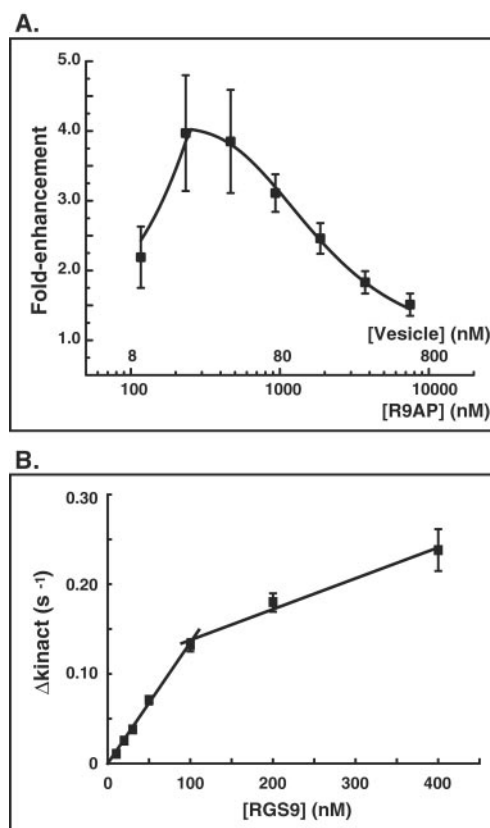


**FIG. 4. Maximum enhancement on RGS9-1 GAP activity by R9AP membrane anchoring.** A, RGS9-1 GAP activity ( $\Delta k_{\text{inact}}$ ) on rhodopsin-only or rhodopsin and R9AP vesicles measured similarly as described for Fig. 3 under a series of different vesicle concentrations (nM): 9.0, 18, 36, 72, 144, 288, and 576. Corresponding rhodopsin concentrations were: 0.38, 0.75, 1.5, 3.0, 6.0, 12.0, and 24.0  $\mu\text{M}$ , and corresponding R9AP concentrations were: 0.12, 0.24, 0.48, 0.96, 1.9, 3.8, and 7.7  $\mu\text{M}$ . Final GST-RGS9-1- $G\beta_5$  concentration was 0.1  $\mu\text{M}$ , and  $G_t$  concentration was 0.2  $\mu\text{M}$  for vesicle concentrations from 9.0 to 36.0 nM and 0.5  $\mu\text{M}$  for vesicle concentrations from 72.0 to 576.0 nM. Enhancement on RGS9-1 GAP activity by R9AP membrane anchoring (*closed squares*) was defined as -fold enhancement =  $\Delta k_{\text{inact}}$  (on rhodopsin and R9AP vesicles)/ $\Delta k_{\text{inact}}$  (on rhodopsin-only vesicles) and was plotted as mean  $\pm$  S.D. against vesicle and R9AP concentrations (on a log scale). Theoretical values were predicted based on the following three assumptions. 1) The binding of  $G_t\alpha$  to the vesicles was independent of the binding of RGS9-1, and the numbers of RGS9-1 per vesicle ( $x$ ) followed the Poisson distribution  $P(x, \mu) = \mu^x e^{-\mu}/x!$ , where  $P(x, \mu)$  is the probability of a vesicle having exactly  $x$  molecules of RGS9-1 when the average number of RGS9-1 molecules per vesicle is  $\mu$ . 2) The dissociation constant  $K_d$  between RGS9-1 and R9AP on the vesicles was much lower than the concentrations used in the experiments so that the concentration of the complex RGS9-1-R9AP is equal to the product of the total formal concentration of R9AP and the fraction exposed on the outside of vesicles when the value of that product is less than the total formal concentration of RGS9-1 and is equal to the total formal concentration of RGS9-1 when the concentration of surface-exposed R9AP exceeds the total RGS9-1. 3) Each  $G\alpha_t$ -GTP stays on the vesicle in which it was originally activated until its bound GTP is hydrolyzed. Thus, the expected -fold enhancement (*smooth line*),  $E$ , is given by:  $E - 1 = (E_{\text{max}} - 1) \times ((\text{total concentration of accessible R9AP})/(\text{total concentration of RGS9-1})) \times [1 - \exp(-\mu)]$  when accessible R9AP  $\leq$  RGS9 and by  $E - 1 = (E_{\text{max}} - 1) \times [1 - \exp(-\mu)]$  when accessible R9AP  $\geq$  RGS9. The values of parameters determined from least-squares fitting were  $E_{\text{max}}$ , 4.0; average radius of the vesicles (used in calculating  $\mu$ ), 272 nm, consistent with the number  $240 \pm 50$  nm calculated from vesicle radii determined by electron microscopy; percent of accessible R9AP (with its soluble domain facing outside), 40%, which is consistent with our result from the binding assays and also suggests that nearly 100% of the R9AP was functional. B, RGS9-1 GAP activity ( $\Delta k_{\text{inact}}$ ) on urea-washed ROS membranes was measured by single turnover assays as described under "Experimental Procedures." The final concentrations of RGS9-1 were 10, 20, 30, 50, 100, 200, and 400 nM. Data were plotted as mean  $\pm$  S.D. and fit to two linear functions (*straight lines*) with slopes of  $1.36 \mu\text{M}^{-1}\text{s}^{-1}$  and  $0.34 \mu\text{M}^{-1}\text{s}^{-1}$ .

tions supports the notion that activated  $G_t$  must interact with RGS9-1 on the membrane on which it was formed for rapid GTP hydrolysis, or, equivalently, that intervesicle exchange of  $G\alpha_t$ -GTP is a slow process relative to the intravesicle encounter of  $G\alpha_t$ -GTP with RGS9-1 and consequent rapid GTP hydrolysis.

Enhancement of the GAP activity of RGS9-1 by membrane anchoring was also observed on urea-washed ROS membranes, in which the endogenous binding sites for RGS9-1 were made accessible to the added recombinant RGS9-1-G $\beta_5$  by denaturation of the endogenous RGS9-1 with urea. We titrated RGS9-1-G $\beta_5$  at a fixed concentration of urea-washed ROS membranes and measured its GAP activity. As reported previously (7), the activity of RGS9-1-G $\beta_5$  increased steeply until the binding sites on the membranes were saturated, and then at higher concentrations the slope decreased (Fig. 4B). The RGS9-1 concentration at the breakpoint was 100 nM, close to the estimated R9AP concentration on the membranes of 60 nM R9AP, assuming a ratio of rhodopsin:R9AP of 1250:1 (3, 21), consistent with the status of R9AP as the endogenous factor providing the binding sites. The enhancement of the GAP activity by membrane binding on these membranes, as calculated from the slopes of the two straight lines in Fig. 4B, was approximately 4-fold, consistent with our results using the reconstituted vesicles. The 4-fold enhancement we observed is considerably lower than the ~70-fold enhancement Lishko *et al.* reported (7), for experiments using similarly prepared membranes. Assuming the  $K_m$  value of 3.2  $\mu$ M reported previously (36), the higher ratio apparently results from a 5-fold higher  $k_{cat}$  value for membrane-enhanced RGS9-1-G $\beta_5$ , and a ~3.5-fold lower  $k_{cat}$  value for RGS9-1-G $\beta_5$  in solution relative to the values we observed. Two differences in the experiments, which may in part account for these discrepancies, are our use of single turnover assays here rather than the steady-state assays used previously (7) and our use of full-length recombinant PDE $\gamma$  in a 1:1 stoichiometric ratio with  $G\alpha_t$  rather than a peptide fragment (amino acid 63–87) derived from it used in high molar excess (7). The use of full-length PDE $\gamma$  necessitates the use of single-turnover assays rather than steady-state assays, because PDE $\gamma$  binds to GDP-form  $G\alpha_t$  tightly enough to inhibit R\*-catalyzed nucleotide exchange (37). In our hands peptides can give very different results from full-length PDE $\gamma$ .<sup>2</sup> It is interesting to consider whether the maximally enhanced GAP activity we observe is sufficient to account for *in vivo* inactivation kinetics. From our experiments (Figs. 4B and 3A), we deduce that the  $k_{cat}/K_m$  value of RGS9-1-G $\beta_5$  when its GAP activity is maximally enhanced either by ROS membranes or reconstituted R9AP-containing vesicles is ~1.3  $\mu$ M<sup>-1</sup>s<sup>-1</sup> at room temperature. Given the *in vivo* RGS9-1 concentration of 3–6  $\mu$ M in mammalian rods (assuming the rhodopsin concentration to be 3–6 mM (38, 39) and the rhodopsin:RGS9-1-G $\beta_5$  ratio to be 1:1000), our  $k_{cat}/K_m$  value would provide recovery times of 160–320 ms, very close to the observed ~200-ms recovery time of mouse rod photoreponses measured in electrophysiological experiments (1). Because of higher temperatures and lower concentrations of chloride ion (an inhibitor of GTP hydrolysis), GTP hydrolysis kinetics likely are more rapid than those observed under our conditions. However, if GTP hydrolysis in rods were 10-fold faster than our results suggest, it would be hard to understand why mammalian cones, which recover less than 10-fold more rapidly than rods, require 10 times higher levels of the RGS9-1-G $\beta_5$  complex (24, 40, 41). Thus, our estimate of maximal RGS9-1 GAP activity, when appropriately corrected for differences in conditions, seems likely to reflect the value attained in

intact rod cells.

In addition to establishing the ability of R9AP membrane anchoring to stimulate GAP activity of RGS9-1, the results presented here using the highly efficient bacterial expression and reconstitution method we have developed will facilitate determination of the role of specific lipids and other molecules of ROS membranes in regulating GAP activity and, possibly, structural studies of the GAP complex.

**Acknowledgments**—We thank the National Center for Macromolecular Imaging for the use of electron microscopy facilities, Dr. Vadim Arshavsky of the Massachusetts Eye and Ear Infirmary for supplying baculovirus encoding RGS9-1-IGRC, and Mathew E. Sowa and Su Gu for technical assistance.

## REFERENCES

- Chen, C. K., Burns, M. E., He, W., Wensel, T. G., Baylor, D. A., and Simon, M. I. (2000) *Nature* **403**, 557–560
- Lyubarsky, A. L., Naarendorp, F., Zhang, X., Wensel, T., Simon, M. I., and Pugh, E. N., Jr. (2001) *Mol. Vis.* **7**, 71–78
- He, W., Cowan, C. W., and Wensel, T. G. (1998) *Neuron* **20**, 95–102
- Makino, E. R., Handy, J. W., Li, T., and Arshavsky, V. Y. (1999) *Proc. Natl. Acad. Sci. U. S. A.* **96**, 1947–1952
- Witherow, D. S., Wang, Q., Levay, K., Cabrera, J. L., Chen, J., Willars, G. B., and Slepak, V. Z. (2000) *J. Biol. Chem.* **275**, 24872–24880
- Ponting, C. P., and Bork, P. (1996) *Trends Biochem. Sci.* **21**, 245–246
- Lishko, P. V., Martemyanov, K. A., Hopp, J. A., and Arshavsky, V. Y. (2002) *J. Biol. Chem.* **277**, 24376–24381
- Cowan, C. W., He, W., and Wensel, T. G. (2000) *Prog. Nucleic Acids Res. Mol. Biol.* **65**, 341–359
- He, W., Lu, L., Zhang, X., El-Hodiri, H. M., Chen, C. K., Slep, K. C., Simon, M. I., Jamrich, M., and Wensel, T. G. (2000) *J. Biol. Chem.* **275**, 37093–37100
- Skiba, N. P., Martemyanov, K. A., Elfenbein, A., Hopp, J. A., Bohm, A., Simonds, W. F., and Arshavsky, V. Y. (2001) *J. Biol. Chem.* **276**, 37365–37372
- Martemyanov, K. A., and Arshavsky, V. Y. (2002) *J. Biol. Chem.* **277**, 32843–32848
- Arshavsky, V. Y., Dumke, C. L., and Bownds, M. D. (1992) *J. Biol. Chem.* **267**, 24501–24507
- Angleton, J. K., and Wensel, T. G. (1993) *Neuron* **11**, 939–949
- Slep, K. C., Kercher, M. A., He, W., Cowan, C. W., Wensel, T. G., and Sigler, P. B. (2001) *Nature* **409**, 1071–1077
- Angleton, J. K., and Wensel, T. G. (1994) *J. Biol. Chem.* **269**, 16290–16296
- Norton, A. W., D'Amours, M. R., Grazio, H. J., Hebert, T. L., and Cote, R. H. (2000) *J. Biol. Chem.* **275**, 38611–38619
- Mou, H., and Cote, R. H. (2001) *J. Biol. Chem.* **276**, 27527–27534
- Calvert, P. D., Govardovskii, V. I., Arshavsky, V. Y., and Makino, C. L. (2002) *J. Gen. Physiol.* **119**, 129–145
- Hu, G., Jang, G. F., Cowan, C. W., Wensel, T. G., and Palczewski, K. (2001) *J. Biol. Chem.* **276**, 22287–22295
- Balasubramanian, N., Levay, K., Keren-Raifman, T., Faurobert, E., and Slepak, V. Z. (2001) *Biochemistry* **40**, 12619–12627
- Hu, G., and Wensel, T. G. (2002) *Proc. Natl. Acad. Sci. U. S. A.* **99**, 9755–9760
- Hay, J. C. (2001) *Exp. Cell Res.* **271**, 10–21
- Harlow, E., and Lane, D. (1988) *Antibodies: a Laboratory Manual*, Cold Spring Harbor Laboratories, pp. 471–510, Cold Spring Harbor, New York
- Sokal, I., Hu, G., Liang, Y., Mao, M., Wensel, T. G., and Palczewski, K. (2003) *J. Biol. Chem.* **278**, 8316–8325
- Papermaster, D. S., and Dreyer, W. J. (1974) *Biochemistry* **13**, 2438–2444
- Litman, B. J. (1982) *Methods Enzymol.* **81**, 150–153
- Parmar, M. M., Edwards, K., and Madden, T. D. (1999) *Biochim. Biophys. Acta* **1421**, 77–90
- Chen, P. S., Toribara, T. Y., and Warner, H. (1956) *Anal. Chem.* **28**, 1756–1758
- Adrian, M., Dubochet, J., Lepault, J., and McDowell, A. W. (1984) *Nature* **308**, 32–36
- Dubochet, J., Adrian, M., Chang, J. J., Homo, J. C., Lepault, J., McDowell, A. W., and Schultz, P. (1988) *Q. Rev. Biophys.* **21**, 129–228
- Struthers, M., Yu, H., and Oprian, D. D. (2000) *Biochemistry* **39**, 7938–7942
- Cowan, C. W., Fariss, R. N., Sokal, I., Palczewski, K., and Wensel, T. G. (1998) *Proc. Natl. Acad. Sci. U. S. A.* **95**, 5351–5356
- Henselman, R. A., and Cusanovich, M. A. (1974) *Biochemistry* **13**, 5199–5203
- Daemen, F. J. M. (1973) *Biochim. Biophys. Acta* **300**, 255–288
- Quick, M., and Wright, E. M. (2002) *Proc. Natl. Acad. Sci. U. S. A.* **99**, 8597–8601
- Skiba, N. P., Hopp, J. A., and Arshavsky, V. Y. (2000) *J. Biol. Chem.* **275**, 32716–32720
- Cowan, C. W., Wensel, T. G., and Arshavsky, V. Y. (2000) *Methods Enzymol.* **315**, 524–538
- Hargrave, P. A., and McDowell, J. H. (1992) *FASEB J.* **6**, 2323–2331
- Pugh, E. N., Jr., and Lamb, T. D. (2000) in *Handbook of Biological Physics: Molecular Mechanisms in Visual Transduction* (Stavenga, D. G., DeGrip, W. J., and Pugh, E. N., eds) Vol. 3, pp. 183–255, Elsevier Science Publishing Co. Inc., New York
- Zhang, X., Wensel, T. G., and Kraft, T. W. (2003) *J. Neurosci.* **23**, 1287–1297

<sup>2</sup> M. E. Sowa and T. G. Wensel, unpublished data.